



Article

The Effect of Electrochemical Surface Properties on Molybdenite Flotation in Seawater

Yang Chen ¹, Na Zhang ^{2,*}  and Haoran Cui ³ ¹ International Mining Research Center, China Geological Survey, Beijing 100083, China; chenyang_imrc@163.com² School of Resources and Safety Engineering, University of Science and Technology Beijing, Beijing 100083, China³ School of Semiconductor and Physics, North University of China, Taiyuan 030051, China; cuihaoran@nuc.edu.cn

* Correspondence: nazhang@ustb.edu.cn

Abstract

Seawater has been widely used in copper–molybdenum flotation plants due to the shortage of fresh water and the high cost of seawater desalination, especially in arid regions. There have been many studies concerning the molybdenite flotation in seawater. Due to the complication of seawater flotation, it is difficult to identify the key factors affecting molybdenite recoveries. It is known that the unique structure of molybdenite plays an important role in molybdenite flotation. The anisotropic property of molybdenite leads to the different surface properties of basal and edge plane surfaces. Electrochemical properties of sulfides have a significant effect on the surface properties which affect the flotation performance. Therefore, it is important to understand the surface electrochemical properties such as surface chemistry, redox processes, and reaction kinetics of molybdenite's two different surfaces in seawater, and to determine what affects the molybdenite flotation behaviors in seawater. In this study, the surface properties of molybdenite basal and edge plane surfaces in both fresh water and seawater were investigated through various electrochemical techniques. Open circuit potential (OCP) measurement indicated that edge plane surfaces were easier to be oxidized than basal plane surfaces. Cyclic voltammetry (CV) studies showed that the basal plane surfaces were stable with a low electrochemical reactivity, while the edge plane surfaces had relatively high electrochemical reactivity. In addition, the redox property of the molybdenite surface was enhanced in seawater, which is a key to the improvement of fine molybdenite flotation in seawater. Electrochemical impedance spectroscopy (EIS) measurements further confirmed the stability of basal plane surfaces and indicated a greater charge transfer ability of edge plane surfaces in seawater. Different molybdenite particle sizes with different basal and edge ratios were applied in the flotation in both fresh water and seawater; the results illustrated that molybdenite flotation was enhanced in seawater especially to fine particles. The flotation and electrochemical studies reveal that the electrochemical reactivity of edge plane surface plays an important role in molybdenite seawater flotation.

Keywords: molybdenite flotation; seawater; basal plane; edge plane; electrochemistry

Academic Editors: Dave Deglon and Luis Vinnett

Received: 6 August 2025

Revised: 15 September 2025

Accepted: 1 October 2025

Published: 3 October 2025

Citation: Chen, Y.; Zhang, N.; Cui, H. The Effect of Electrochemical Surface Properties on Molybdenite Flotation in Seawater. *Minerals* **2025**, *15*, 1049. <https://doi.org/10.3390/min15101049>

Copyright: © 2025 by the authors. Licensee MDPI, Basel, Switzerland. This article is an open access article distributed under the terms and conditions of the Creative Commons Attribution (CC BY) license (<https://creativecommons.org/licenses/by/4.0/>).

1. Introduction

Molybdenite is a unique sulfide mineral and the primary source to extract molybdenum. Normally, molybdenite is associated with copper sulfides such as chalcopyrite. Ap-

proximately 50% of molybdenum production comes from porphyry copper–molybdenum ores [1]. Due to fresh water shortages, the application of seawater is becoming a trend in the beneficiation of Cu-Mo minerals in arid regions [2]. The flotation using seawater is very complex with both advantages and challenges for molybdenite flotation. It was found that the compression of electrical double layers was responsible for the improvement in molybdenite floatability when using saline water [3,4]. In addition, Castro and Laskowski proposed that bubble coalescence was reduced in saline water, which promoted molybdenite flotation [5]. Besides Na^+ and Cl^- , there are still many other ions such as SO_4^{2-} , Mg^{2+} , Ca^{2+} , and CO_3^{2-} . These ions are collectively called secondary ions, and they have different effects on molybdenite flotation [6]. It was identified that the hydrolysable ions in seawater such as magnesium and calcium ions can depress molybdenite flotation at high pH [7,8].

It is known that molybdenite has a layered structure with two types of surfaces, which are basal and edge plane surfaces [9]. Previous studies showed that during the breakage of the crystalline structure, edge planes were generated from the breakup of Mo-S covalent bonds, while the formation of basal planes was due to the breakage of S-Mo-S layers which are bonded through weak van der Waals interactions, which determine that the basal plane surface energy is very low while that of the edge plane is much higher [10]. This explains the reason why platelet-shaped fragments are generally produced during grinding [11,12]. In addition, many previous studies demonstrate that edge plane surfaces are hydrophilic while basal plane surfaces are hydrophobic without exception. The edge/basal ratio increases with the decrease in particle sizes [13–15]. Therefore, the hydrophobicity of coarse particles with predominant basal plane surfaces are higher. For fine particles, the hydrophobicity of molybdenite reduces significantly with more edge plane surface generation [16].

Electrochemical technology is highly sensitive to subtle changes on the surface properties of sulfides, and recent studies showed that electrochemical properties of sulfides played a key role in flotation [17,18]. Sulfide minerals can also be oxidized to form hydrophobic sulfur-rich species or hydrophilic sulfoxo species on the surfaces and therefore display different flotation behaviors [19]. It has been validated that in fresh water, the floatability of molybdenite was highly related to its hydrophobic basal plane surfaces and hydrophilic edge plane surfaces [20]. However, it is unclear whether the characteristics of molybdenite surfaces can still be maintained in seawater, as seawater is highly conductive and contains various ions. The electrochemical properties of molybdenite's two surfaces have not been well understood, especially in seawater. Considering that flotation is a water-intensive process and the flotation efficiency is highly dependent on water type, it is necessary to investigate how the electrochemical properties of molybdenite surfaces change and affect the flotation behaviors of molybdenite in seawater.

In this work, the electrochemical properties of both surfaces of molybdenite were studied by using bulk molybdenite electrode samples. Tests were conducted in both supporting electrolyte and seawater, adopting different electrochemical testing methods, including OCP, CV, and EIS. Then the flotation tests of different molybdenite particle sizes in fresh water and seawater were conducted to validate the results. The findings of the molybdenite surface electrochemical properties in this study will provide a better understanding of molybdenite flotation behaviors in seawater.

2. Materials and Methods

2.1. Materials

Molybdenite ore of a high grade used in this study was supplied by GEOdiscoveries, Australia. The detailed chemical compositions of the sample are shown in Table 1. According to the analysis, the molybdenite sample has a Mo grade of 58.3% and S grade of 39.5%. These results were in line with previous studies using pure molybdenite samples

and further confirmed that the molybdenite ore sample was of high purity [21–23]. For electrochemical studies, high-quality molybdenite crystals were employed to prepare basal and edge plane electrodes. A smooth and flat basal plane surface was achieved by peeling off the top layer of molybdenite crystals carefully using tweezers. For the edge plane surface, the crystals were cut perpendicular to the layered structure using a diamond saw, thereby exposing the required edge planes [24]. For flotation tests, the molybdenite ore was crushed and sieved to obtain 3.35–0.6 mm fraction and then stored at a low temperature before grinding.

Table 1. Chemical compositions of the molybdenite ore in this work.

	Species Present (wt.%)											
	Al ₂ O ₃	Bi	CaO	Co	Cu	Fe	Mo	Pb	S	SiO ₂	Ti	Zn
Molybdenite	0.13	0.23	0.07	0.01	0.06	0.14	58.3	0.06	39.5	1.52	-	0.01

The seawater used in this study was prepared according to the composition of the process water used in a copper–molybdenum plant in Chile which uses seawater. The composition of the process water was measured, and the results are shown in Table 2. The sulfate ions were analyzed turbidimetrically, and the chloride ions were analyzed colorimetrically. The other chemical compositions of seawater were determined by ICP-MS (Inductively coupled plasma-Mass Spectrometry). It is worth noting that the composition of this water may be different from that of natural seawater due to evaporation and cycle use. The synthetic seawater was prepared according to the procedures in other studies [25]. DI (deionized) water and seawater were applied in flotation to investigate the effect of water types on molybdenite flotation directly.

Table 2. The main chemical composition of the synthetic seawater in this study and the main composition of natural seawater (mg/L).

Type	Ca ²⁺	K ⁺	Mg ²⁺	Na ⁺	SO ₄ ^{2−}	Cl [−]	CO ₃ ^{2−} /HCO ₃ [−]
Synthetic seawater	3494	588	2897	14,236	8447	30,300	341
Average seawater	400	280	1272	10,556	2649	18,980	140

Diesel and Methyl Isobutyl Carbinol (MIBC) were employed as the collector and the frother in the flotation tests, respectively. The pH in flotation was adjusted by 1M sodium hydroxide (NaOH). In electrochemical studies, 0.01M KCl (AR grade) was prepared and used as the supporting electrolyte. Water used in the electrochemical tests was purified with a Milli-Q system.

2.2. Electrochemical Studies

In electrochemical studies, the molybdenite surface properties in supporting electrolyte (0.01M KCl) and seawater were investigated through open circuit potential (OCP), cyclic voltammetry (CV), and electrochemical impedance spectroscopy (EIS). These measurements were conducted on a CHI 920D electrochemical workstation and a 200 mL three-electrode electrochemical cell. An Ag/AgCl (3M KCl) electrode and a Pt electrode were used as the reference and counter electrode, respectively. The working electrode was either a basal plane electrode or an edge plane electrode depending on the experimental objectives. The potential recorded was against the Ag/AgCl reference electrode and converted to the potential against the standard hydrogen electrode (SHE) by adding 220 mV in the results [26]. The objective of the electrochemical experiments in this study was to investigate the surface properties of molybdenite basal and edge plane surfaces in both fresh water and

seawater and help to better understand the flotation behaviors of molybdenite. Therefore, nitrogen was not used in electrochemical experiments.

The working electrode was refreshed to generate fresh surface and then inserted to the solutions prior to each measurement. OCP measurement was conducted before CV and EIS measurements and time for OCP was 1200 s to reach stabilization. The final OCP was used as the initial potential in CV tests, and the scanning potential range was from -0.5 to $+0.5$ V (against Ag/AgCl) with the initial positive-scanning direction. Different switching potentials were not applied in this study as the anodic and cathodic switching potentials in this study were pre-determined by the potential range in molybdenite flotation. The CV experiments conducted in this scanning range helped to provide information of molybdenite surface redox reactions which could explain the molybdenite flotation behaviors in fresh water and seawater. The scan rate was 0.01 V/s and five cycles were performed. The third cycle was adopted because the peak shape and intensity became stable. The initial and final frequencies for EIS measurements were 0.01 and $10,000$ Hz, respectively. The obtained impedance data was analyzed using Zview software (v.40h) and presented as Bode plots and Nyquist plots.

2.3. Grinding and Flotation

Single mineral flotation with different molybdenite particle sizes was conducted. A 100 g prepared sample was ground using a laboratory rod mill. To obtain molybdenite with a d_{80} of $106\ \mu\text{m}$ and $53\ \mu\text{m}$, 8.9 kg of stainless steel rods were used, respectively, with grinding times of 10 min and 20 min. A Malvern sizer 2000 (Malvern, UK) was employed to measure the molybdenite particle size distributions and the results are shown in Figure 1. The amount of water used during the grinding process was 150 mL, and the type of water was consistent with that used in the flotation. The collector (diesel, 1.5 g) was added directly into the mill. After grinding, flotation was carried out in a 1.5 L JK batch flotation cell. The pulp density during the flotation process was approximately 6.7% (by weight, solid content). The frother (MIBC, 300 g/t) was added then, with the conditioning time being 2 min. The pH value during flotation was adjusted by NaOH and maintained at 7.5. The stirring speed was fixed at 1000 revolutions per minute (rpm), and the air flow rate was $3\ \text{dm}^3/\text{min}$. The products scraped at cumulative times of 1, 3, 6, and 10 min were collected as four types of concentrates. Pulp chemistry during flotation including pH and Eh was monitored by a pH-mV-Temp meter. Flotation products including concentrates and tailings were filtrated, dried, and weighted. As a single mineral flotation, the flotation recoveries were determined based on Equation (1), where R is the flotation recovery, m_1 and m_2 are the mass of minerals in the concentrates and tailings. Each flotation test was repeated three times and the average flotation results were reported with 95% CI (confidence interval) error bars.

$$R = \frac{m_1}{m_1 + m_2} \times 100\% \quad (1)$$

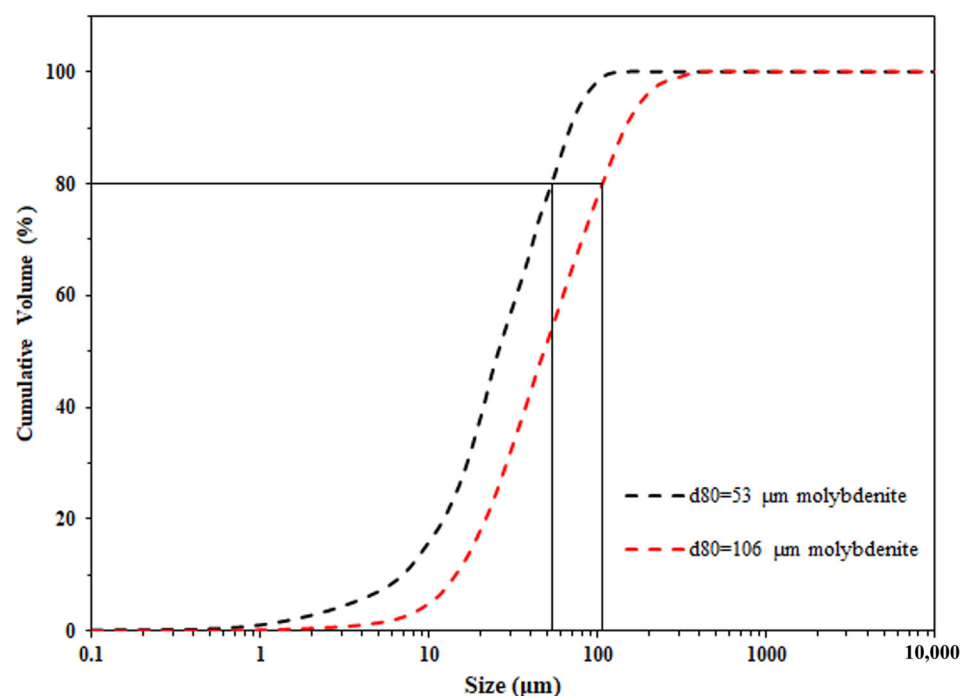


Figure 1. Particle size distributions of 106 μm and 53 μm molybdenite.

3. Results and Discussion

3.1. Electrochemical Studies

3.1.1. Open Circuit Potential Measurements

OCP was employed to determine the surface conditions of molybdenite and to obtain a surface which was stabilized in the target solution for the follow-up tests as well. The OCP vs. time curves of the molybdenite basal plane electrode in 0.01M KCl and seawater are shown in Figure 2a, while the OCP vs. time curves of the molybdenite edge plane electrode in 0.01 M KCl and seawater are presented in Figure 2b. Table 3 illustrates the initial OCP of the basal plane and edge plane electrodes in the supporting electrolyte and seawater. It can be observed that the initial OCP of the basal plane in the supporting electrolyte was 0.29 V and the value in seawater was 0.24 V. For the edge plane electrode, the initial OCP in the supporting electrolyte was 0.27 V and it was 0.17 V in seawater. The initial OCP was measured immediately after immersing the electrodes in solutions, which could represent the surface conditions of the electrodes. The different values of OCPs in the supporting electrolyte and seawater resulted from the lower DO (dissolved oxygen) in seawater than in fresh water. The higher initial OCPs of the basal plane than that of the edge plane indicated that surface oxidation in the basal plane was less than that in the edge plane.

Table 3. Initial OCP (vs. SHE/mV) of molybdenite basal and edge electrodes in the supporting electrolyte (0.01M KCl) and seawater.

Electrode	Supporting Electrolyte	Seawater
MoS ₂ -Basal	293	239
MoS ₂ -Edge	270	167

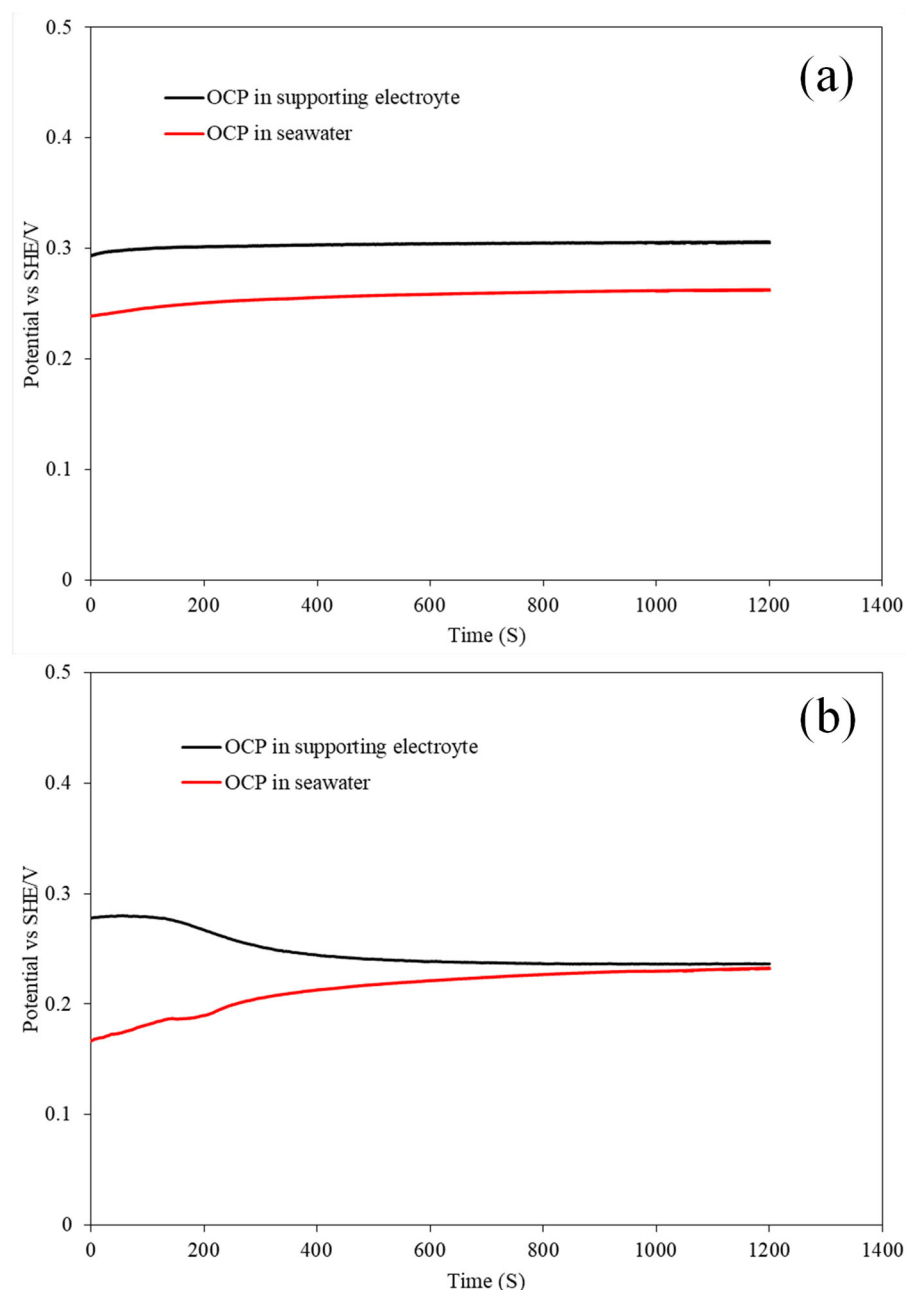


Figure 2. OCP (vs. SHE/V) vs. time of molybdenite basal (a) and edge (b) electrodes in the supporting electrolyte and seawater.

It can be seen from Figure 2a that the OCP of the basal electrode reached stabilization quickly after measurement and the OCP did not have a significant shift over time. The behaviors of the basal plane in the supporting electrolyte and seawater indicated that the basal plane surface is relatively stable in both fresh water and seawater due to its low electrochemical reactivity. However, the edge plane surface took a longer time to reach stabilization in the OCP measurement in both the supporting electrolyte and seawater, and the longer time to reach stabilization indicated higher electrochemical activity. Normally, the shifts in OCPs can be caused by the solution pH, surface redox reactions, dissolution, and adsorption. In the supporting electrolyte, the OCP of the edge plane shifting negatively was attributed to the relatively strong dissolution of pre-immersion oxide and the formation of the soluble species HMoO_4^- and MoO_4^{2-} [10,27]. However, the OCP of the edge plane electrode shifting positively in seawater indicated that the electrical double layer (EDL) structure at the edge

electrode surface might be modified in seawater. Previous studies have suggested that the adsorption of positively charged species could result in the positive shift in OCP, which is in agreement with the conclusion that the adsorption of cations such as Mg and Ca in seawater occurred on edge planes in the forms of cations and hydrated cations [28]. In conclusion, the OCP measurement indicated that the basal plane surface had less surface oxidation and it was stable in the supporting electrolyte and seawater. In addition, the different OCPs of the edge plane surface in the supporting electrolyte and seawater illustrate different surface conditions of the edge plane in fresh water and seawater.

3.1.2. Cyclic Voltammetry Measurements

The specific information about the surface redox properties was investigated by CV measurements considering that CV measurements can provide the electrochemical reactions occurring on molybdenite basal and edge plane surfaces exposed to various solutions. Figure 3 indicated the results of the CV measurements of the MoS₂ basal plane electrode in both the supporting electrolyte and seawater. From Figure 3, it can be seen that the basal electrode did not show any inherent redox peaks in the supporting electrolyte, which indicated that the basal plane surface of molybdenite had a low electrochemical reactivity, and it was not responsible for the surface redox. The CV curve of the basal electrode in seawater further indicated that in seawater, the redox could not happen on the basal plane surface with no redox peaks observed. The current density of the CV curve in seawater was slightly higher than that in the supporting electrolyte, owing to the higher conductivity in seawater than the supporting electrolyte.

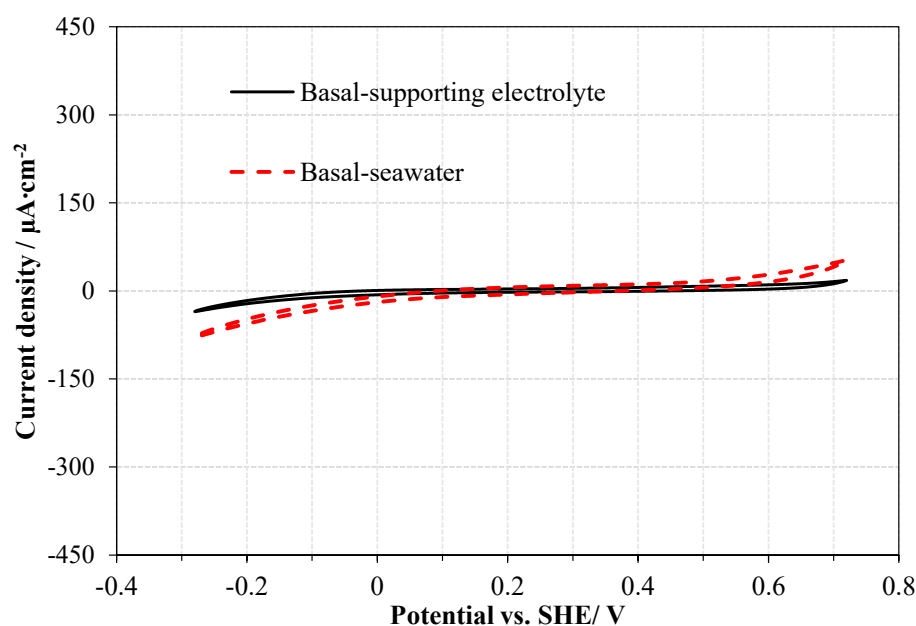


Figure 3. CV curves of MoS₂ basal electrodes in supporting electrolyte (0.01M KCl) and seawater (positive-scanning, 3rd cycle, scan rate 0.01 V/s).

The CV results of the edge planes in different solutions are shown in Figure 4. Anodic and cathode peaks were indicated with peak A₁, peak C₁, and peak C₂, respectively. Peak A₁ at around 0 V was attributed to the oxidation of sulfide to sulfur (S⁰), the oxidation of Mo, and the further oxidation of sulfur to sulfate as well, as shown in Equations (2) and (3) [11,29]. It is noteworthy that S⁰ here was not a single species but a series of the oxidation products of S^{2−} in MoS₂ (e.g., S_n^{2−}). The peak C₁ at around 0.1 V was attributed to the reduction in higher oxidation state Mo to Mo⁴⁺ (Equation (4)). The peak C₂ commencing from −0.1 V represented the regeneration of HS[−]/S^{2−} (Equation (5)) [30].

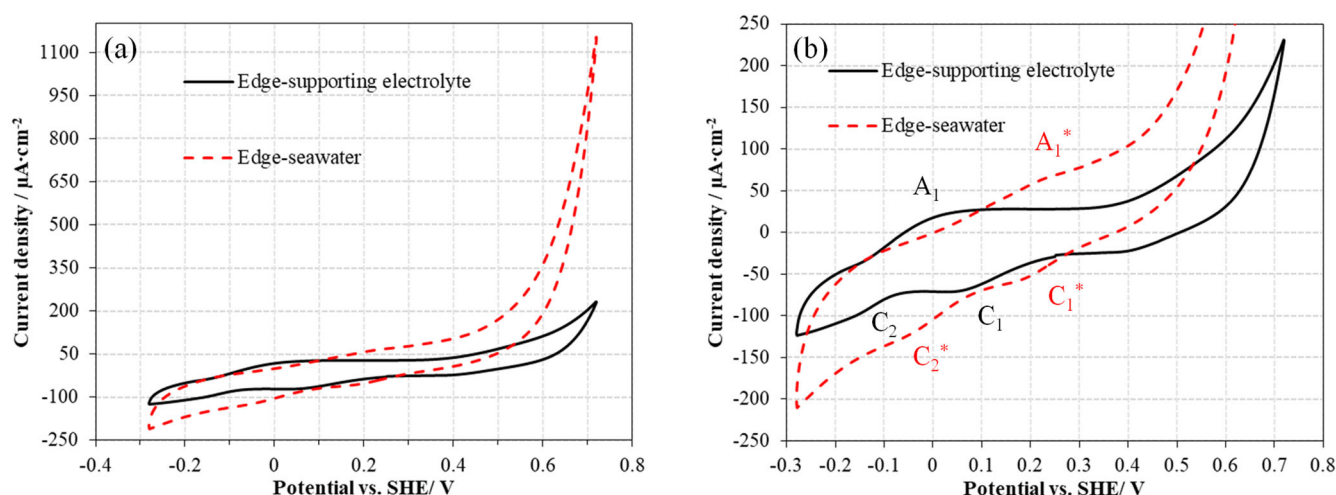
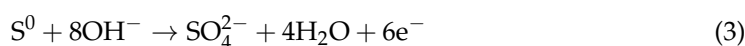
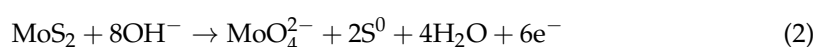


Figure 4. CV curves of MoS₂ edge electrodes in the supporting electrolyte and seawater: complete voltammograms (a), and magnified view of peaks (b) (positive-scanning, 3rd cycle, scan rate 0.01 V/s).

The peaks of the edge plane surface in seawater were also indicated in Figure 4 (red peaks with asterisks). However, these peaks in seawater had different peak positions and current densities compared with those in the supporting electrolyte, which was due to the lower oxygen amount and the higher current density in seawater. Peak A₁* commencing from 0.1 V was attributed to the formation of sulfur species and oxidation of Mo. Meanwhile, the shift in peak A₁ position originated from the less dissolved oxygen in seawater. The significant higher current intensity of peak A₁* than peak A₁ suggested that more aggressive oxidation occurred on the edge plane surface in seawater. The cathodic peak C₁* starting from 0.3 V represents the reformation of Mo⁴⁺ but the higher starting potential of peak C₁* indicated that the reduction in higher oxidation state Mo was easier in seawater. The more pronounced current intensity of cathodic peak C₂* than peak C₂ resulted from the generation of more hydrosulfides or sulfides in seawater. From the results of the CV curves, it is clear that the basal plane itself was not involved in any redox reaction in both fresh water and seawater, suggesting a low electrochemical reactivity of the basal plane. In addition, the redox reactions occurred on the edge plane surface, and aggressive redox products were more likely to form on the edge plane surface in seawater, which is related to the flotation behavior changes in fresh water and seawater.



3.1.3. Electrochemical Impedance Spectroscopy Measurements

The electrode process kinetics and surface conditions of molybdenite were investigated by EIS measurement. The Nyquist plot and Bode plot of the basal electrode in the supporting electrolyte and seawater are shown in Figure 5, while these plots for the edge plane electrode are shown in Figure 6. The Nyquist plot is a curve which shows the imaginary impedance versus real impedance. The Bode plot consists of two curves, one describing the relationship between impedance and frequency while the other represents the phase angle as a function of frequency. A physical model of the electrical double layer for molybdenite electrodes in an electrolyte solution was proposed in Figure 7a. Previous

studies have shown that the surface of fresh molybdenite is negatively charged under all alkaline pH conditions. According to the Stern model, when an electrode is inserted into an electrolyte solution, the surface of the electrode becomes charged, triggering the rearrangement of charges, ions, and dipoles. The redistribution of charges promotes the formation of an electric double layer and generates a potential difference at the interface. To maintain electrical neutrality, the solution near the surface carries an equal number of counter-ions. The trajectory of the specific adsorption ion center determines the position of the inner layer, while the trajectory of the hydrated ion center is referred to as the outer layer. The electric double layer between the electrode/electrolyte interface appears as two planes with equal and opposite charges, electrically equivalent to a capacitor. Based on this physical model, an equivalent circuit for the electrochemical system is proposed, as shown in Figure 7b. This equivalent circuit consists of a resistor R_s (solution resistance) connected in series with a parallel circuit, which includes a capacitor C_{dl} (double-layer capacitance) and a resistor R_{ct} known as the charge transfer (or polarization) resistance. Zview software was employed to fit the electrochemical impedance spectroscopy (EIS) data using the equivalent circuit proposed in Figure 7b. The extract electrochemical parameters are listed in Table 4.

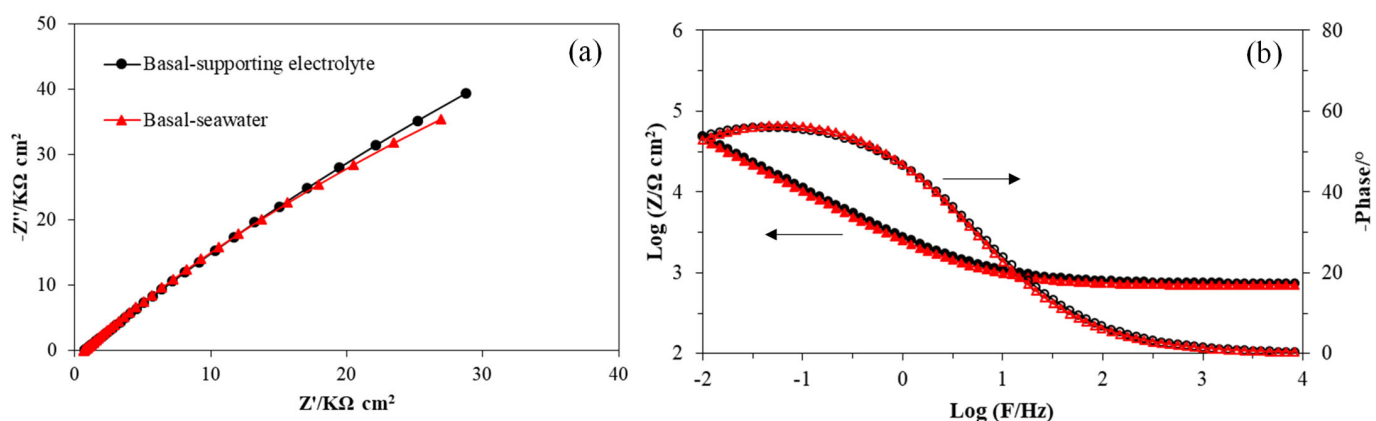


Figure 5. Impedance of MoS₂ basal electrode in the supporting electrolyte (black lines) and seawater (red lines) presented in the Nyquist plot (a) and the Bode plot (b).

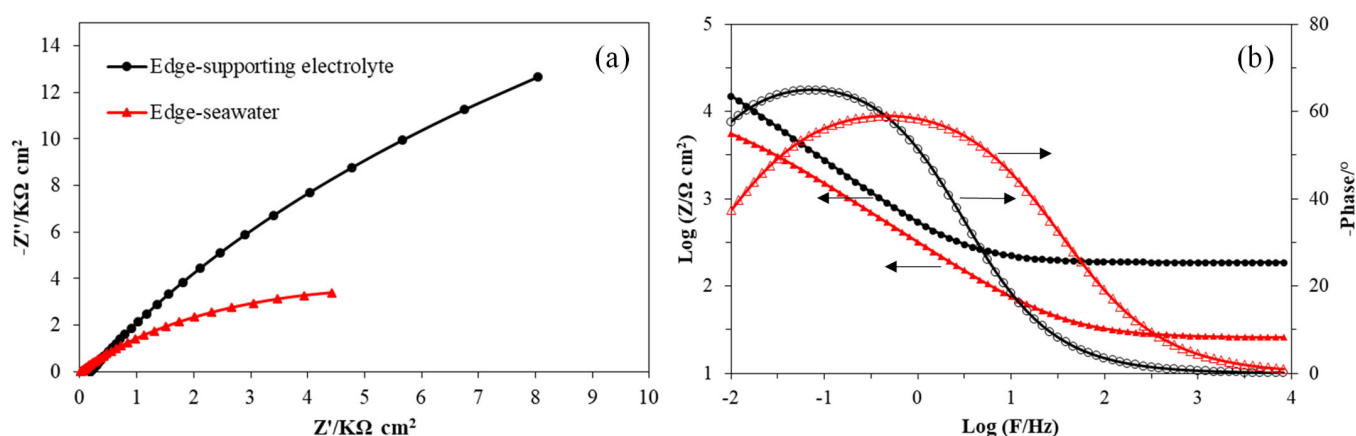


Figure 6. Impedance of MoS₂ edge electrode in the supporting electrolyte (black lines) and seawater (red lines) presented in the Nyquist plot (a) and the Bode plot (b).

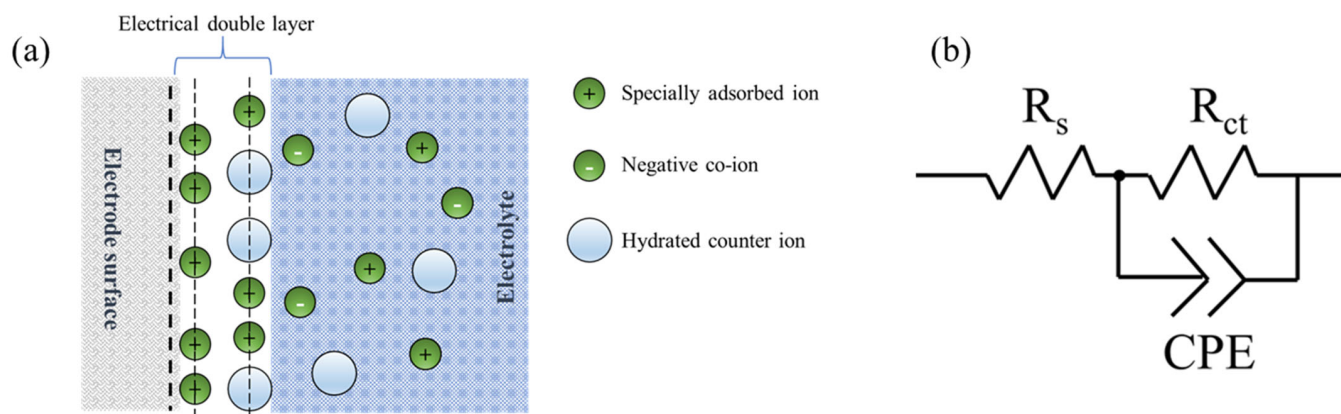


Figure 7. A physical model of the electrical double layer for molybdenite electrodes in an electrolyte solution (a) and the equivalent circuit for fitting the EIS data (b).

Table 4. Electrochemical impedance spectroscopy parameters for MoS₂ edge and basal electrodes in supporting electrolyte and seawater.

	$R_s \ \Omega \text{ cm}^2$	$R_{ct} \text{ k}\Omega \text{ cm}^2$	$C_{dl} \ \mu\text{F cm}^{-2}$	n
Basal-Supporting electrolyte	745.4	354.4	128.3	0.68
Basal-Seawater	696.7	350.5	132.9	0.68
Edge-Supporting electrolyte	184.9	65.5	529.3	0.78
Edge-Seawater	25.7	11.3	870.9	0.71

The experimental errors are as follows: R_s is 0.5%–0.7%, R_c is 1.1%–1.9% for t , and C_{dl} is 0.6%–0.8%.

From Figure 5 it can be seen that the spectra of basal electrodes in the supporting electrolyte and seawater overlapped most, which was in line with the observation from CV curves that the electrochemical properties of the basal plane surface of molybdenite were stable in both fresh water and seawater. In Table 4, most parameters for the basal plane in the supporting electrolyte were similar except that the solution resistance R_s in seawater was lower than that in supporting electrolyte. This is understandable due to the higher electrolyte concentration and higher conductivity in seawater.

However, the Nyquist plot in Figure 6 clearly shows different semicircles and the Bode plot in Figure 6 also suggests different Bode magnitude and phase diagrams, which indicated that the electrode/electrolyte interface of the molybdenite edge plane surface had significant changes in seawater and the supporting electrolyte [31]. It was found that in the same solution, R_s of the basal plane and edge plane electrodes were different. This difference might originate from different electrodes used in EIS tests (basal and edge plane electrodes). Different electrodes have different OCPs even in the same solution, and different OCPs applied in EIS may result in different fitted R_s . For the same electrode (e.g., R_s of the edge electrode in Table 4), the R_s in different solutions showed a clear difference and the results indicated the different solution resistances between fresh water and seawater. In the Nyquist plot, the radius of the capacitive reactance loops can show the resistance of a mineral surface. The longer radius of the loop in the supporting electrolyte indicated that the surface resistance of the edge plane surface in supporting electrolyte was greater than that in seawater [32]. In addition, the surface resistance was also revealed in Table 4. The charge transfer resistance R_{ct} for the edge electrode in supporting electrolyte was 65.5 k $\Omega \text{ cm}^2$, which was much higher than that in seawater (11.3 k $\Omega \text{ cm}^2$). The R_{ct} was inversely proportional to electrochemical reactivity, thus the lower R_{ct} in seawater of the edge plane surfaces suggested a higher electrochemical reactivity. This also agreed with the findings in CV studies that more intense redox occurred on edge plane surfaces in seawater. The EIS results in Table 4 also show a difference in the capacitance of the

electrical double layer (C_{dl}) of the edge plane electrode in the supporting electrolyte and seawater. The higher C_{dl} of the edge plane electrode in seawater also suggested that the electrochemical reactivity of edge plane surfaces was improved in seawater. In addition, the slight decreased factor n in seawater might be due to the formation of more redox products on edge plane surfaces which affected the homogeneity of the electrode surface.

3.2. Flotation Tests

The flotation of 106 μm and 53 μm molybdenite in both DI water and seawater was conducted, and the results are shown in Figure 8, respectively. As can be seen from Figure 8, in DI water, the final recovery of molybdenite was 91%, showing an excellent flotation performance. Specifically, the recovery of molybdenite with a particle size of 53 μm was 53% at the end of flotation in DI water, which was obviously lower than that of molybdenite with a particle size of 106 μm under the same flotation condition. This is expected, as the floatability of molybdenite is related to its particle size. The flotation results were in line with the previous studies that the coarse particles floated fast and completely, while the fine particles floated slowly and incompletely. It is well-known that the flotation of molybdenite is determined by its hydrophobic basal planes, and as the particle size decreases, the proportion of the basal planes of molybdenite also decreases. Therefore, the floatability of molybdenite with a particle size of 53 μm was lower than that of molybdenite with a particle size of 106 μm . After conducting the flotation tests in DI water, molybdenite flotation in seawater was carried out and the results are also presented in Figure 8. The overall recovery of 106 μm molybdenite was about 93%. As a result, the flotation of molybdenite at 106 μm in seawater had a slight rise compared to that in DI water. Meanwhile, the 53 μm molybdenite recoveries were increased to 70% in seawater, which is a significant improvement compared with that in DI water. The molybdenite flotation results were in line with the previous studies by others, in which the molybdenite flotation recoveries of different size particles were improved using seawater [33,34].

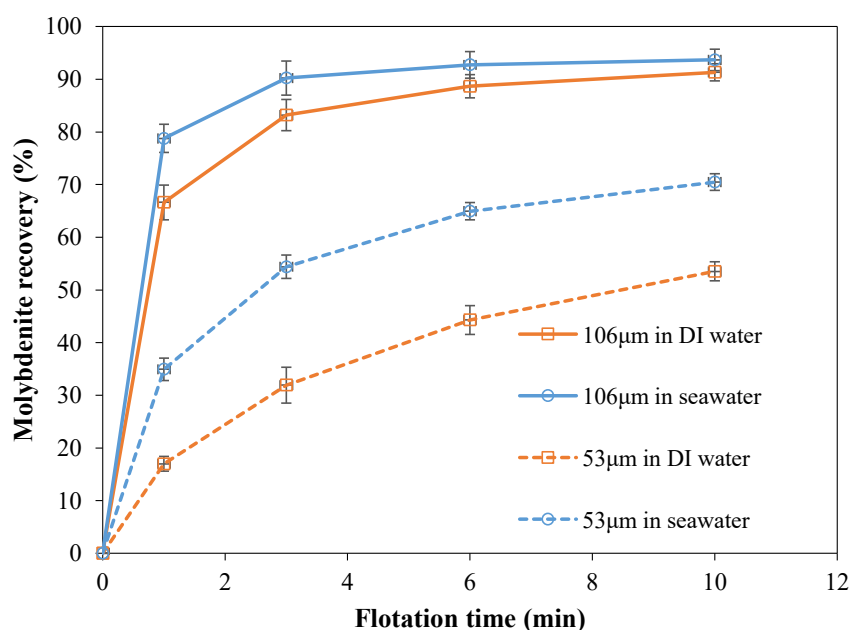


Figure 8. The 106 μm molybdenite and 53 μm molybdenite flotation recovery in DI water and seawater.

It is known that molybdenite has an anisotropic surface property, and different hydrophobicity for different crystal planes. In this electrochemical study, it is clarified that the basal plane has a more stable surface property in both fresh water and seawater, while the edge plane surfaces are more reactive and the electrochemical reactivity is improved

in seawater from the results in OCP, CV, and EIS measurement. In other words, edge plane surfaces are responsible for the different flotation performance in fresh water and seawater, especially considering that 53 μm molybdenite particles with more edge plane surfaces became more floatable in seawater but 106 μm molybdenite particles did not. OCP measurements indicated that in seawater, the edge plane surfaces have more oxidation, with lower initial OCP. Cyclic voltammetry measurements further indicated that the redox reactions occurred on the edge plane surface, and redox products (such as the oxidation of sulfide to sulfur (S^0) shown in Equation (2) were more likely to form on edge plane surfaces in seawater, due to the higher electrolyte concentration and higher conductivity. According to the Nernst equation (see Equation (6)), E_h is determined by the activities of oxidized (a_{Ox}) and reduced species (a_{Red}). In fresh water, sulfur (S^0) was difficult to form on molybdenite surfaces as pulp potential was higher than the required electrochemical potential of Reaction (2). As a result, sulfate species preferred to be formed. In seawater, due to the presence of considerable sulfate ions, the further oxidation of sulfur (S^0) to sulfate was actually inhibited. EIS also suggested that some oxidation products were formed on edge plane surfaces which affected the homogeneity of the electrode surface. Based on the flotation results, in electrochemical studies, the surface changes on both two orientation surfaces of molybdenite in seawater can be summarized. There was no significant change on the molybdenite basal plane surface in seawater; the basal plane surface retained its hydrophobicity in seawater due to its inertness. It agrees well with the flotation results that 106 μm and 53 μm molybdenite recoveries did not decline in this and previous studies. In addition, the flotation results demonstrated that in seawater, 106 μm molybdenite flotation recovery had a small increase while 53 μm molybdenite flotation improved a lot. The improvement of molybdenite flotation, especially 53 μm molybdenite, demonstrates that the edge plane surfaces played a key role in the seawater flotation, owing to the high edge-to-basal ratio of finer particles. For 106 μm molybdenite, basal planes dominated the flotation, resulting in only a slight increase in seawater flotation recovery. It is worth noting that changes in the surface properties of sulfides (such as hydrophobicity) depend on changes in surface composition. Electrochemical studies in this work showed that there were some redox reactions occurring on the edge plane surfaces of molybdenite. In addition, hydrophobic species such as sulfur species (S^0) were more likely to form and adsorb on due to the significant electrochemical activity of the edge planes and the presence of a large amount of sulfate ions in seawater, which significantly improved the flotation efficiency of molybdenite with a particle size of 53 μm .

$$E_h = E^0 - \frac{RT}{nF} \ln \frac{a_{\text{Red}}}{a_{\text{Ox}}} \quad (6)$$

where E^0 is the standard electrode potential, R is the gas constant, T is the absolute temperature, n is the number of electrochemical equivalents per mole, F is the Faraday constant, and a_{Red} and a_{Ox} are the activities of the reduced form and oxidized form, respectively.

4. Conclusions

The electrochemical results indicated that the basal plane surface had a low electrochemical reactivity due to its inertness, while the edge plane surface had a relatively high electrochemical reactivity with redox reactions occurring on this surface in supporting electrolyte. The electrochemical studies conducted in seawater indicated that the basal plane surface remained stable; however, the electrochemical reactivity of the edge planes was further enhanced in seawater and more hydrophobic species were formed in the edge planes through redox reactions. These findings in electrochemical studies show the difference in two surfaces of molybdenite in electrochemical reactivity, and the reactivity gap

was boosted in seawater, resulting in the different flotation behaviors of molybdenite in fresh water and seawater.

Author Contributions: Y.C.: Methodology; Data curation; Formal analysis; Writing—original draft; Writing—review and editing. N.Z.: Formal analysis; Methodology; Review and editing. H.C.: Conceptualization; Resources. All authors have read and agreed to the published version of the manuscript.

Funding: This research was funded by the Fundamental Research Funds for the Central Universities, China [No. FRF-TP-22-116A1].

Data Availability Statement: The data that support the findings of this study are available upon request by contact with the corresponding author.

Conflicts of Interest: The authors declare no conflicts of interest.

References

1. Castro, S.; Lopez-Valdivieso, A.; Laskowski, J.S. Review of the flotation of molybdenite. Part I: Surface properties and floatability. *Int. J. Miner. Process.* **2016**, *148*, 48–58. [\[CrossRef\]](#)
2. Moreno, P.A.; Aral, H.; Cuevas, J.; Monardes, A.; Adaro, M.; Norgate, T.; Bruckard, W. The use of seawater as process water at Las Luces copper–molybdenum beneficiation plant in Taltal (Chile). *Miner. Eng.* **2011**, *24*, 852–858. [\[CrossRef\]](#)
3. Peng, Y.; Zhao, S.; Bradshaw, D. Role of saline water in the selective flotation of fine particles. *Water Miner. Process.* **2012**, *15*, 61–71.
4. Pan, L.; Yoon, R.-H. Effects of electrolytes on the stability of wetting films: Implications on seawater flotation. *Miner. Eng.* **2018**, *122*, 1–9. [\[CrossRef\]](#)
5. Castro, S.; Miranda, C.; Toledo, P.; Laskowski, J.S. Effect of frothers on bubble coalescence and foaming in electrolyte solutions and seawater. *Int. J. Miner. Process.* **2013**, *124*, 8–14. [\[CrossRef\]](#)
6. Jeldres, R.I.; Arancibia-Bravo, M.P.; Reyes, A.; Aguirre, C.E.; Cortes, L.; Cisternas, L.A. The impact of seawater with calcium and magnesium removal for the flotation of copper–molybdenum sulphide ores. *Miner. Eng.* **2017**, *109*, 10–13. [\[CrossRef\]](#)
7. Hirajima, T.; Suyantara, G.P.W.; Ichikawa, O.; Elmahdy, A.M.; Miki, H.; Sasaki, K. Effect of Mg^{2+} and Ca^{2+} as divalent seawater cations on the floatability of molybdenite and chalcopyrite. *Miner. Eng.* **2016**, *96–97*, 83–93. [\[CrossRef\]](#)
8. Chen, Y.; Chen, X.; Peng, Y. The effect of sodium hydrosulfide on molybdenite flotation in seawater and diluted seawater. *Miner. Eng.* **2020**, *158*, 106589. [\[CrossRef\]](#)
9. Becker, U.; Rosso, K.M.; Weaver, R.; Warren, M.; Hochella, M.F. Metal island growth and dynamics on molybdenite surfaces. *Geochim. Cosmochim. Acta* **2003**, *67*, 923–934. [\[CrossRef\]](#)
10. Lu, Z.; Liu, Q.; Xu, Z.; Zeng, H. Probing Anisotropic Surface Properties of Molybdenite by Direct Force Measurements. *Langmuir* **2015**, *31*, 11409–11418. [\[CrossRef\]](#)
11. Tan, S.M.; Ambrosi, A.; Sofer, Z.; Huber, Š.; Sedmidubský, D.; Pumera, M. Pristine Basal- and Edge-Plane-Oriented Molybdenite MoS₂ Exhibiting Highly Anisotropic Properties. *Chem. A Eur. J.* **2015**, *21*, 7170–7178. [\[CrossRef\]](#)
12. Heising, J.; Kanatzidis, M.G. Structure of restacked MoS₂ and WS₂ elucidated by electron crystallography. *J. Am. Chem. Soc.* **1999**, *121*, 638–643. [\[CrossRef\]](#)
13. Xie, L. Probing Surface Heterogeneity, Electrochemical Properties and Bubble-Solid Interaction Mechanisms of Sulfide Minerals in Flotation. Ph.D. Thesis, University of Alberta, Edmonton, Canada, 2017.
14. Zanin, M.; Ametov, I.; Grano, S.; Zhou, L.; Skinner, W. A study of mechanisms affecting molybdenite recovery in a bulk copper/molybdenum flotation circuit. *Int. J. Miner. Process.* **2009**, *93*, 256–266. [\[CrossRef\]](#)
15. Wang, H.; Gu, G.-H.; Fu, J.-G.; Chen, L.; Hao, Y. Study of the interfacial interactions in the molybdenite floatation system. *J. China Univ. Min. Technol.* **2008**, *18*, 82–87. [\[CrossRef\]](#)
16. Yang, B.; Song, S.; Lopez-Valdivieso, A. Morphology of Hydrophobic Agglomerates of Molybdenite Fines in Aqueous Suspensions. *Sep. Sci. Technol.* **2015**, *50*, 1560–1564. [\[CrossRef\]](#)
17. Chanturiya, V.A.; Krasavtseva, E.A.; Makarov, D.V. Electrochemistry of Sulfides: Process and Environmental Aspects. *Sustainability* **2022**, *14*, 11285. [\[CrossRef\]](#)
18. Wang, J.; Zeng, H. Recent advances in electrochemical techniques for characterizing surface properties of minerals. *Adv. Colloid Interface Sci.* **2020**, *288*, 102346. [\[CrossRef\]](#)
19. Chander, S. Electrochemistry of sulfide flotation: Growth characteristics of surface coatings and their properties, with special reference to chalcopyrite and pyrite. *Int. J. Miner. Process.* **1991**, *33*, 121–134. [\[CrossRef\]](#)
20. Yang, B.; Song, S.; Lopez-Valdivieso, A. Effect of Particle Size on the Contact Angle of Molybdenite Powders. *Miner. Process. Extr. Metall. Rev.* **2014**, *35*, 208–215. [\[CrossRef\]](#)

21. Wang, E.; Wan, H.; Qu, J.; Yi, P.; Bu, X. Inhibiting Mechanism of High pH on Molybdenite Flotation. *Exp. DFT Study. Miner.* **2024**, *14*, 663.
22. Zhang, Q.D.; Li, X.L.; Hu, Z.F.; Gao, B.W.; Liu, C. Study on Floatation Separation of Molybdenite and Talc Based on Crystal Surface Anisotropy. *Separations* **2025**, *12*, 123. [[CrossRef](#)]
23. Chao, Y.D.; Li, S.L.; Gao, L.H.; Sun, L.J.; Li, L.N.; Chai, N.; Cao, Y.J. Enhanced Flotation Recovery of Fine Molybdenite Particles Using a Coal Tar-Based Collector. *Minerals* **2021**, *11*, 1439. [[CrossRef](#)]
24. Miki, H.; Matsuoka, H.; Hirajima, T.; Suyantara, G.P.W.; Sasaki, K. Electrolysis Oxidation of Chalcopyrite and Molybdenite for Selective Flotation. *Mater. Trans.* **2017**, *58*, 761–767. [[CrossRef](#)]
25. Kester, D.R.; Duedall, I.W.; Connors, D.N.; Pytkowicz, R.M. Preparation of artificial seawater 1. *Limnology and oceanography* **1967**, *12*, 176–179. [[CrossRef](#)]
26. Mu, Y.; Peng, Y.; Lauten, R.A. Electrochemistry aspects of pyrite in the presence of potassium amyl xanthate and a lignosulfonate-based biopolymer depressant. *Electrochim. Acta* **2015**, *174*, 133–142. [[CrossRef](#)]
27. Wang, J.; Xie, L.; Lu, Q.; Wang, X.; Wang, J.; Zeng, H. Electrochemical investigation of the interactions of organic and inorganic depressants on basal and edge planes of molybdenite. *J. Colloid Interface Sci.* **2020**, *570*, 350–361. [[CrossRef](#)] [[PubMed](#)]
28. Wan, H.; Yang, W.; Cao, W.; He, T.; Liu, Y.; Yang, J.; Guo, L.; Peng, Y. The Interaction between Ca^{2+} and Molybdenite Edges and Its Effect on Molybdenum Flotation. *Minerals* **2017**, *7*, 141. [[CrossRef](#)]
29. Hirajima, T.; Miki, H.; Suyantara, G.P.W.; Matsuoka, H.; Elmahdy, A.M.; Sasaki, K.; Imaizumi, Y.; Kuroiwa, S. Selective flotation of chalcopyrite and molybdenite with H_2O_2 oxidation. *Miner. Eng.* **2017**, *100*, 83–92. [[CrossRef](#)]
30. Spevack, P.A.; McIntyre, N. A Raman and XPS investigation of supported molybdenum oxide thin films. 1. Calcination and reduction studies. *J. Phys. Chem.* **1993**, *97*, 11020–11030. [[CrossRef](#)]
31. Mu, Y.; Peng, Y.; Lauten, R.A. The depression of copper-activated pyrite in flotation by biopolymers with different compositions. *Miner. Eng.* **2016**, *96–97*, 113–122. [[CrossRef](#)]
32. Ertekin, Z.; Pekmez, K.; Ekmekçi, Z. Evaluation of collector adsorption by electrochemical impedance spectroscopy. *Int. J. Miner. Process.* **2016**, *154*, 16–23. [[CrossRef](#)]
33. Lucay, F.; Cisternas, L.; Gálvez, E.; López-Valdivieso, A. Study of the natural floatability of molybdenite fines in saline solutions. Effect of gypsum precipitation. *Miner. Metall. Process. J.* **2015**, *32*, 203–208. [[CrossRef](#)]
34. Yepsen, R.; Roa, J.; Toledo, P.G.; Gutiérrez, L. Chalcopyrite and Molybdenite Flotation in Seawater: The Use of Inorganic Depressants to Reduce the Depressing Effects of Micas. *Minerals* **2021**, *11*, 539. [[CrossRef](#)]

Disclaimer/Publisher’s Note: The statements, opinions and data contained in all publications are solely those of the individual author(s) and contributor(s) and not of MDPI and/or the editor(s). MDPI and/or the editor(s) disclaim responsibility for any injury to people or property resulting from any ideas, methods, instructions or products referred to in the content.